



ELSEVIER

Journal of Electron Spectroscopy and Related Phenomena 71 (1995) 73–77

JOURNAL OF  
ELECTRON SPECTROSCOPY  
and Related Phenomena

# Resonant photoemission versus incoherent superposition of Auger and photoemission signals

M.F. López\*,<sup>1</sup>, A. Gutiérrez, C. Laubschat, G. Kaindl

*Institut für Experimentalphysik, Freie Universität Berlin, Arnimallee 14, D-14195 Berlin-Dahlem, Germany*

First received 10 February 1994; in final form 17 August 1994

## Abstract

The angle-resolved resonant photoelectron spectra of Ni and Ce metals are reported. On  $M_{III}$  resonance, the intensity of the 6-eV satellite of Ni is found to be independent of the angle of emission relative to the  $\vec{E}$ -vector of the exciting light, while the valence-band photoemission (PE) intensity follows a  $\cos^2$  behavior as expected for PE. In contrast to Ni, the enhanced Ce4f PE signal on  $N_{IV,V}$  resonance also varies according to  $\cos^2$ . This shows that the resonant enhancement of the 6-eV Ni satellite is mainly due to a secondary Auger decay, whereas in case of the Ce4f signal it reflects resonant photoemission.

**Keywords:** ARPES; Auger; Incoherent superposition; PES; Resonant photoemission

## 1. Introduction

Valence-band photoemission (PE) spectra of Ni metal are characterized by a satellite structure at  $\approx 6$  eV below the Fermi energy ( $E_F$ ), which has been interpreted as a two-hole bound state separated by a large on-site Coulomb interaction from the main valence-band emission [1–4]. This satellite exhibits a strong enhancement when the photon energy is varied across the  $M_{III}$  absorption threshold at  $\approx 67$  eV. This phenomenon has been assigned to a strong Fano-type resonance [5–15], and is explained by configurational mixing of two different final states, a continuum state represented

by the outgoing photoelectron and a discrete state produced by transition of a core electron to an unoccupied bound state. Because the second process is strongly energy dependent, the probability of transition to the intermixed final state varies dramatically when tuning the photon energy across the core threshold, causing the well-known Fano profile in the photoionization cross-section. Since the probability for resonant PE depends critically on the strength of configuration interaction, and therefore on the localization of the core-excited state, the question arises whether the signal observed in resonant PE reflects exclusively this excitation process or is due in part to a secondary decay process of the excited state. Only in the first case can the spectral features be interpreted as resonant PE; in the second case an incoherent superposition of PE and Auger signals occurs. The second mechanism was first discussed more

\* Corresponding author.

<sup>1</sup> Present address: Laboratoire, pour l'Utilisation du Rayonnement Electromagnetique Université Paris-Sud, Bâtiment 209D, 91405 Orsay, France.

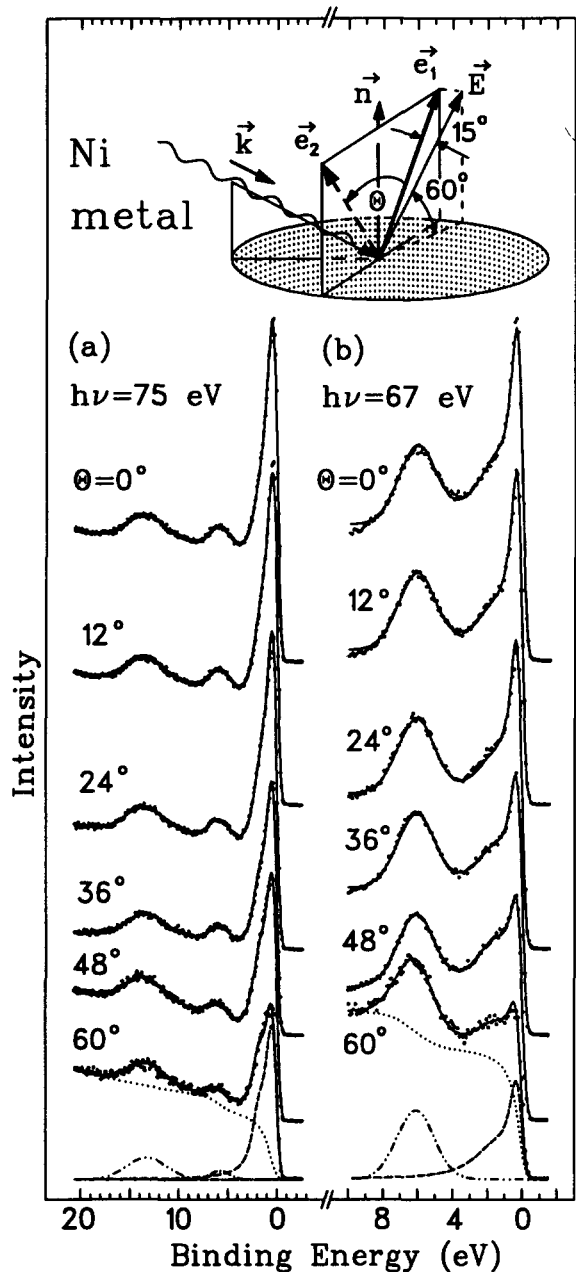


Fig. 1. Photoelectron spectra of Ni metal taken at photon energies of (a) 75 eV (non-resonant) and (b) 67 eV (on-resonance). The solid lines through the data points represent the results of least-squares fits (see text). For  $h\nu = 75$  eV, the dash-dotted subspectrum represents the 6-eV PE satellite, the dashed subspectrum the valence-band signal, and the dash-double-dotted curve the super-Coster–Kronig Auger contribution. For  $h\nu = 67$  eV, the dashed subspectrum represents the PE signal and the dash-double-dotted curve the 6-eV feature. The dotted curves

than ten years ago [16] but has been neglected since then in the literature.

In a recent paper [17] it was shown that the photoelectron spectra of Ni metal and of CuO at the  $L_{III}$  thresholds have to be described by an incoherent superposition of an intense  $L_3M_{4,5}M_{4,5}$  Coster–Kronig Auger signal with a relatively weak PE signal. It has to be tested whether an analogous mechanism causes the well-known resonant enhancement of the 6-eV valence-band satellite in the photoelectron spectrum of Ni metal at the  $M_{III}$  threshold, and whether similar processes affect resonant PE in rare-earth systems.

In this publication, we show that the resonant enhancement of the 6-eV valence-band satellite of Ni metal is caused mainly by superposition of PE with an incoherent super Coster–Kronig (SCK) Auger signal. This conclusion is reached on the basis of the measured angular dependence of the electron-emission intensity recorded as a function of the angle of emission with respect to the  $\vec{E}$ -vector of the photon beam. Though the intensity of the valence-band PE signal of Ni metal varies roughly according to a  $\cos^2$  law, the intensity of the 6-eV satellite on resonance is found to be independent of the emission angle, as expected for an incoherent Auger process. This clearly shows that the so-called resonant PE enhancement of the 6-eV valence-band satellite of Ni metal, which has been taken for granted for almost fifteen years, is based on a misinterpretation of the observed phenomenon. In contrast to Ni, resonant PE in rare-earth (RE) systems behaves completely differently. The 4f PE signal measured at the Ce4d  $\rightarrow$  4f giant resonance, for example, reveals the characteristic angular dependence expected for PE. This

describe integral backgrounds. Note the large width of the Auger emission at  $h\nu = 75$  eV, which is due to the superposition of both the  $M_3VV$  and the  $M_2VV$  transitions, whereas at  $h\nu = 67$  eV only the  $M_3VV$  Auger transition contributes to the resonance phenomenon. The inset shows the geometrical arrangement of the experiment:  $\vec{E}$  and  $\vec{k}$  represent the direction of the electric field and the momentum of the photons, respectively,  $\vec{n}$  denotes the normal to the surface and  $\vec{e}_{1,2}$  shows the directions of the collected electrons. Electrons emerging normal to the surface were collected at an angle  $\theta = 30^\circ$ . This geometry was chosen to assure the same surface sensitivity at  $\theta = 0^\circ$  and  $\theta = 60^\circ$  ( $\vec{e}_1$  and  $\vec{e}_2$ , respectively).

distinctively different behavior is due to the stronger localization of the 4f states in Ce compared to the 3d states in Ni.

## 2. Experimental

The measurements were performed at the TGM-1 beamline of the Berliner Elektronenspeicherring für Synchrotronstrahlung (BESSY) using a VSW-ARIES angle-resolved electron spectrometer with an electron-acceptance cone of  $\pm 2^\circ$ . The photoelectrons were collected at different angles with respect to the  $\vec{E}$ -vector. The geometrical arrangement as well as the definition of the emission angle  $\theta$  are shown inset in Fig. 1. Polycrystalline samples were used to avoid angular dispersion effects. The surfaces of the samples were cleaned by scraping with a diamond file. Oxygen contamination was monitored via O2p PE at  $h\nu = 52$  eV and was found to be negligible. During the experiments, the pressure in the experimental chamber was better than  $2 \times 10^{-10}$  Torr.

## 3. Results and discussion

Fig. 1 shows the valence-band spectra of Ni metal taken at (a)  $h\nu = 75$  eV (non-resonance) and (b)  $h\nu = 67$  eV (on-resonance) as a function of the angle of emission  $\theta$ . The non-resonant spectra reveal three main features: (i) the Ni3d valence-band PE signal at binding energies between  $E_F$  and  $\approx 3$  eV; (ii) the PE satellite at a binding energy of  $\approx 6$  eV; and (iii) an Auger signal at a binding energy of  $\approx 13.5$  eV. In order to take into account possible intensity variations of the spectra due to changes in geometry when  $\theta$  is varied, the non-resonant spectra were normalized to equal intensities of the Auger signals. This is justified, as the Auger emission can be assumed to be isotropic for a polycrystalline sample.

To arrive at a quantitative estimate for the intensity variations as a function of  $\theta$  of the valence-band PE signal and of the 6-eV PE satellite, the spectra were analyzed by least-square fits. To this end, the Auger signal (dash-double-dotted sub-

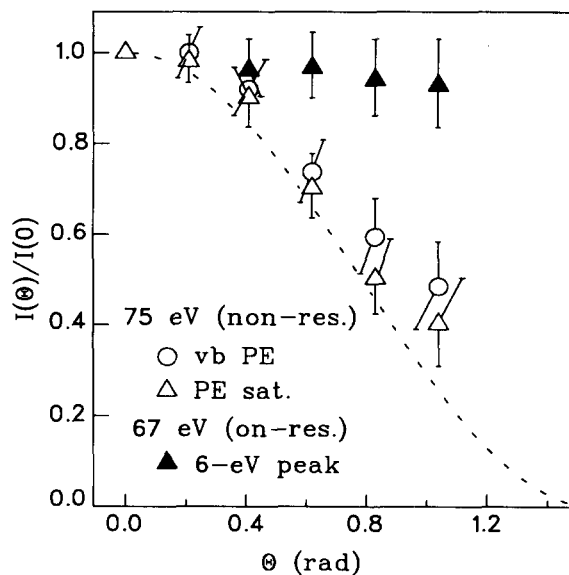


Fig. 2. Angular dependences of the intensities of the valence-band PE signal (open circles) and the 6-eV PE satellite (open triangles) in the non-resonant spectra ( $h\nu = 75$  eV). The intensities of the 6-eV feature in the on-resonance spectra ( $h\nu = 67$  eV) are given by the filled triangles. The dashed curve represents a  $\cos^2\theta$  behavior.

spectrum) and the 6-eV PE satellite (dash-dotted curve) were modelled by Gaussians, and the valence-band signal was simulated by a superposition of two Lorentzians at binding energies (BE) of 0.3 and 1.9 eV, respectively (the sum of both is represented by the dashed curves in Fig. 1(a)). Inelastically scattered electrons were accounted for by an integral background (dotted). Note that the intensity of this background is not expected to change with  $\theta$ , since an initial angular dependence will be lost owing to multiple scattering of the secondary electrons. The resulting intensity variations as a function of  $\theta$  of the non-resonant valence-band and satellite emission are indicated in Fig. 2 by open symbols. As expected for PE, both intensities vary roughly as  $\cos^2\theta$ .

In order to normalize the on-resonance spectra of Ni metal in Fig. 1(b), we assumed the same angular dependence of the intensity of the valence-band emission as in the non-resonant case. The on-resonance spectra were therefore normalized to valence-band intensities equal to those in the non-resonant spectra. This normaliza-

tion procedure is based on an analogous least-squares fit analysis of the on-resonance spectra as described above for the non-resonant case. The solid lines in Fig. 1(b) represent the results of this fit analysis, with the dashed subspectrum representing the valence-band PE signal and the dash-double-dotted subspectrum the 6-eV feature. For the normalization procedure, only the main valence-band component at 0.3 eV BE was considered. The second component at 1.9 eV BE revealed a weaker angular variation of its intensity, possibly because of superposition with an energy-loss feature and — in the case of the on-resonance spectra — with an additional Auger signal [8]. The resulting intensity variation of the 6-eV feature of Ni metal as a function of  $\theta$  is given by the filled triangles in Fig. 2. It is apparent that the intensity of this peak is almost independent of  $\theta$ , in sharp contrast to the  $\cos^2\theta$  behavior of the PE satellite in the non-resonance spectra. Thus, the 6-eV peak on resonance behaves like an Auger signal and cannot be described as a resonant PE feature. At this point we are not able to assert whether this Auger signal is due to a normal Auger process, in which the excited electron is not coupled to the Auger decay, or to a resonant Auger process, in which there is a coherence between the excitation event and the Auger decay. If the resonant Auger process is isotropic, as the normal Auger process is, the intensity enhancement of the 6-eV satellite may originate from a mixture of both processes.

If we assume that this peak is made up of two components, an isotropic Auger emission signal A and a PE component B, the latter with the characteristic  $\cos^2\theta$  angular dependence, the relative intensities of the two components are readily obtained from the observed angular dependence (filled triangles in Fig. 2). In this way, on the basis of the measured spectral intensities, a value of the ratio of the intensity of the PE component B to that of the valence-band emission in the on-resonance spectra of  $0.1 \pm 0.2$  is obtained, in agreement with the value of  $0.09 \pm 0.02$  obtained from the PE satellite intensities in the non-resonance spectra. This means that, within the limits of error, there is no resonant enhancement of the PE satellite. The seeming intensity increase

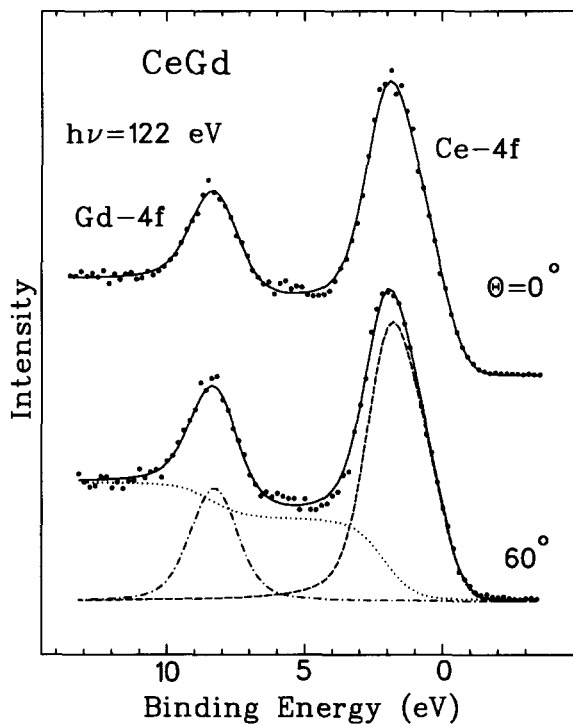


Fig. 3. On-resonance photoelectron spectra of CeGd taken at photon energies of 122 eV for two values of  $\theta$ . The dash-dotted subspectrum represents the Gd4f emission and the dashed subspectrum the on-resonance Ce4f emission. The dotted curve describes the integral background. The intensity scale is arbitrary and different for both spectra.

of the 6-eV satellite is therefore due to the Auger component A, with an intensity of  $0.6 \pm 0.2$  relative to the valence-band emission. This means that the component A, assigned to an Auger (normal or resonant) process, is predominantly responsible for the observed resonant enhancement of the 6-eV photoelectron peak.

To check whether related processes contribute also to the resonant PE spectra of rare-earth materials, we studied the alloy CeGd at the Ce  $4d \rightarrow 4f$  giant resonance at  $h\nu = 122$  eV. Fig. 3 displays the respective valence-band spectra taken at two angles of emission  $\theta$ . The spectra consist of a strong emission feature close to  $E_F$  reflecting the resonantly enhanced emission from Ce4f states plus a weaker component at a binding energy of 8 eV corresponding to the non-resonant Gd4f<sup>7</sup> PE signal; the latter can be used for normalization purposes. As is obvious from even the raw data,

the ratio of intensities of the on-resonance Ce4f emission to that of the non-resonant Gd4f emission does not change with  $\theta$ . The non-resonant Gd4f line is a normal photoemission line and, according to Fermi's golden rule in the dipolar approximation, has a  $\cos^2 \theta$  angular dependence. This means that, for  $\theta = 60^\circ$ , the intensity decreases by a factor of 4 with respect to  $\theta = 0^\circ$  (not seen in Fig. 3, where the spectra are arbitrarily scaled). Because the ratio between the on-resonance Ce4f line and the non-resonant Gd4f line is the same in both cases, we can conclude that the Ce4f line behaves also as a function of  $\cos^2 \theta$ . Therefore the angular dependence of the resonantly enhanced Ce4f emission behaves like a PE signal, in contrast to that of the resonantly enhanced 6-eV Ni satellite.

#### 4. Summary

We have shown that the established interpretation [5–15] of the resonant enhancement of the 6-eV satellite in the valence-band photoelectron spectrum of Ni metal at the  $M_{III}$  threshold is incorrect. The observed phenomenon is dominated by a SCK Auger decay process as seen before in the related case of resonant photoelectron spectra taken at the  $L_{III}$  threshold [17]. Our present results support a related view put forward more than ten years ago [16], which has been totally neglected in the literature. The situation is different in resonant PE from rare-earth materials, where the resonantly enhanced signal reflects a true PE process. The main difference between the systems is the degree of localization of the discrete excited state. While the excited 4f state in the case of Ce is highly localized, the more bandlike character of the Ni3d states favors a decay of the core-excited state by a secondary SCK process. The present results are crucial for a correct interpretation of the photoelectron spectra taken in threshold regions, in particular for transition-metal systems, since they show that not all enhanced spectral

features reflect resonant PE, but competing secondary processes can be important.

#### Acknowledgments

This work was supported by the Bundesminister für Forschung und Technologie, project 05-5KEAXI-3/TP01, and the Deutsche Forschungsgemeinschaft, project Ka564/2-2. Two of the authors (M.F.L. and A.G.) thank the Spanish Ministerio de Educación y Ciencia for financial support. Expert assistance by the staff of BESSY is gratefully acknowledged.

#### References

- [1] D.R. Penn, Phys. Rev. Lett., 42 (1979) 921.
- [2] A. Liebsch, Phys. Rev. Lett., 43 (1979) 1431.
- [3] W. Eberhardt and E.W. Plummer, Phys. Rev. B, 21 (1980) 3245.
- [4] N. Mårtensson and B. Johansson, Phys. Rev. Lett., 45 (1980) 482.
- [5] U. Fano, Phys. Rev., 124 (1961) 1866.
- [6] C. Guillot, Y. Ballu, J. Paigné, J. Lecante, K.P. Jain, P. Thiry, R. Pinchaux, Y. Pétrouff and L.M. Falicov, Phys. Rev. Lett., 39 (1977) 1632.
- [7] M. Iwan, F.J. Himpsel and D.E. Eastman, Phys. Rev. Lett., 43 (1979) 1829.
- [8] J. Barth, G. Kalkoffen and C. Kunz, Phys. Lett., 74A (1979) 360.
- [9] R. Clauberg, W. Gudat, E. Kisker, E. Kuhlmann and G.M. Rothberg, Phys. Rev. Lett., 47 (1981) 1314.
- [10] M.R. Thuler, R.L. Benbow and Z. Hurych, Phys. Rev. B, 26 (1982) 669.
- [11] L.C. Davis and L.A. Feldkamp, Phys. Rev. Lett., 44 (1980) 673.
- [12] T. Jo, A. Kotani, J.C. Parlebas and J. Kanamori, J. Phys. Soc. Jpn., 52 (1983) 2581.
- [13] Y. Sakisaka, T.N. Rhodin and P.A. Dowben, Solid State Commun., 49 (1984) 563.
- [14] Y. Sakisaka, T. Komeda, M. Onchi, H. Kato, S. Masuda and K. Yagi, Phys. Rev. B, 36 (1987) 6383.
- [15] O. Björneholm, J.N. Andersen, C. Wigren, A. Nilsson, R. Nyholm and N. Mårtensson, Phys. Rev. B, 41 (1990) 10408.
- [16] M.M. Traum, N.V. Smith, H.H. Farrell, D.P. Woodruff and D. Norman, Phys. Rev. B, 20 (1979) 4008.
- [17] M.F. López, A. Höhr, C. Laubschat, M. Domke and G. Kaindl, Europhys. Lett., 20 (1992) 357.